

# **Integrating satellite altimetry and key observations: what we've learned, and what's possible with new technologies**

**By**

Mark Bourassa, Dudley Chelton, Paolo Cipollini, Raf Ferrari, Lee-Lueng Fu, Boris Galperin, Sarah Gille, Huei-Ping Huang, Patrice Klein, Nikolai Maximenko, Rosemary Morrow, Bo Qiu, Ernesto Rodriguez, Rob Scott, Detlef Stammer, Remi Tailleux, Carl Wunsch

The advent of high accuracy satellite altimetry in the 1990's brought the first global view of ocean dynamics, which together with a global network of supporting observations brought a revolution in understanding of how the ocean works (Fu and Cazenave, 2001). At present a constellation of flying satellite missions routinely provides sea level anomaly, sea winds, sea surface temperature (SST), ocean colour, etc. with mesoscale resolution (50km to 100km, 20 to 150 days) on a near global scale. Concurrently, *in situ* monitoring is carried out by surface drifters, Argo floats, moorings, sea gliders as well as ship-borne CTD and XBT (to measure profiles of temperature and salinity), and ADCP (to measure current velocity profiles).

This global observational system allowed observational oceanography to develop into an essentially quantitative science. This became possible because 1) the accuracy and volume of observations exceeded critical values, 2) numerous studies demonstrated good agreement between independent datasets, and critically 3) the data resolution crossed the threshold of revealing much of the mesoscale in two-dimensions, when previously it was only revealed in one-dimension along satellite ground tracks (Stammer, 1997) with wide gaps in between. Fortuitously computing power kept pace allowing basin scale numerical ocean models to cross the threshold of revealing the mesoscale around the turn of the century (Smith et al., 2000). The mesoscale is characterized by the most energetic motions and strong nonlinear interactions, issuing in a more complex range of phenomena. Below in Part I we present some highlights of this development. In Part II we describe future prospects, and Part III provides a reminder of the importance of maintaining continuity of high-quality observations.

This white paper comes at a critical juncture in ocean observing. While the utility of the observing network is firmly grounded in the success of the past, and technological advances promise the possibility of substantial gains, we still lack the commitment for sustained funding of even the existing observing network. We wish to express herein our sincere concern for the future of ocean observing, and in particular the satellite altimeter and supporting observations (especially scatterometer and drifter data).

## **PART I: PROGRESS IN OCEANOGRAPHY FROM SATELLITE ALTIMETRY AND SUPPORTING OBSERVATIONS**

### **A. Global view of linear Rossby waves**

i) *Theoretical understanding of complexity of linear Rossby waves*

The linear standard normal-mode theory (LST hereafter) was, prior to satellite altimetry, the main framework for oceanic Rossby waves. Some important features of the standard Rossby wave modes are: 1) that they are all stable and energetically decoupled; 2) that they have a period that increases with latitude up to several years at high-latitude, 3) that they are nearly nondispersive at low wavenumbers (i.e. equal group and phase speeds at long wavelengths), 4) that they are strongly dispersive at high wavenumbers, with the zonal phase speed approaching zero as the wavenumbers increase.

Nearly all these characteristics appear to be inconsistent to various degrees with those of westward propagating signals (WPS) observed in satellite altimeter data collected over the past 17 years. Given the gross simplifications of the LST, it's perhaps not surprising that LST does not fit the observations well. But interestingly Chelton and Schlax (1996) (CS96 hereafter) found observed phase speeds, as measured by the Radon Transform (RT hereafter), to be systematically faster by a factor of up to two to three than the longwave phase speed predicted by the LST for the first baroclinic mode at mid- and high-latitudes. Furthermore, Fu and Chelton (2001) suggest that actual westward propagation is nearly nondispersive throughout the whole wavenumber range. These results prompted much theoretical work over the past decade. The main results are that the background zonal mean flow (Killworth et al., 1997) and rough topography (Tailleux and McWilliams, 2001) are each, on their own, able to bring theoretical phase speeds closer to CS96's RT phase speed estimates in the long wave limit, although room for improvement exists. The best agreement is achieved by combining the effects of a background mean flow and variable bottom topography (Killworth and Blundell, 2003, 2004, 2005), but theoretical issues remain open. With regard to dispersion, the current understanding is that only the background mean flow can potentially make Rossby waves nondispersive at high-wavenumbers (Tailleux and Maharaj, 2009). Maharaj et al. (2009) find secondary peaks in the RT, which they interpreted as evidence of higher-baroclinic modes, though another possibility would be nonlinear eddies, see section B below.

## ii) *Climatic importance of linear Rossby waves*

The ocean impacts human society through marine resources and Earth's climate. The tropical Pacific phenomenon of El Nino-Southern Oscillation provides a well-known example whose coupled atmosphere-ocean nature and global impacts have been appreciated since the 1980s. Below we describe another important example, the Pacific Decadal Oscillation (PDO), one of the largest climate signals in the North Hemisphere (Mantua et al., 1997). Here too observationally driven ocean science was essential for developing our understanding of the coupled climate system.

It is now well established that the large-scale, wind-induced sea surface height (SSH) variability is controlled by baroclinic Rossby wave dynamics (e.g., Miller et al. 1998; Deser et al. 1999; Seager et al. 2001; Schneider et al. 2002; Qiu and Chen 2005; Taguchi et al. 2007). Specifically, the large-scale SSH changes can be hindcast by integrating the anomalous wind-stress curl forcing along the Rossby wave characteristics along a latitude line from the eastern boundary.

Figure 1a shows the altimeter-derived SSH anomaly signals averaged in the latitudinal band of 32-34°N in the North Pacific Ocean as a function of time and longitude. Notice that the decadal

SSH changes in the eastern North Pacific can be qualitatively explained by the wind stress curl variability associated with the PDO, with centre of action around 160°W. Specifically, when the PDO index is positive (see Fig.1c), the Aleutian Low intensifies and shifts southward, and this works to generate negative SSH anomalies near 160°W in the eastern North Pacific through surface wind stress driven Ekman divergence. The opposite is true when the PDO index is negative: wind-induced Ekman convergence in this case results in regional, positive SSH anomalies near 160°W. SSH anomalies generated in the eastern North Pacific tend to propagate westward at the speed of baroclinic Rossby waves of  $\sim 3.8$  cm/s, taking many years to cross the basin to reach the Kuroshio Extension east of Japan.

Figure 1b shows the time-longitude plot of the SSH anomaly field in the same 32-34°N band modeled by the linear Rossby wave model with the use of the monthly wind stress curl data from the National Centers for Environmental Prediction-National Center for Atmospheric Research (NCEP-NCAR) reanalysis (Kistler et al. 2001). As expected, the Rossby wave model captures well all of the large-scale SSH anomaly signals that change sign on decadal timescales. The linear correlation coefficient between the observed and modeled SSH anomaly fields is  $r = 0.45$  and this coefficient increases to 0.53 when only the interannual SSH signals are retained in Fig.1a. This quantitative comparison confirms the notion that the decadal Kuroshio Extension modulations detected by the satellite altimeter data over the past 15 years are initiated by the incoming SSH anomaly signals generated by the PDO-related wind forcing in the eastern North Pacific.

## **B. The Nonlinear Threshold**

While the revolution in the 1990s came from the first global monitoring of the ocean, the revolution of the present decade has come from crossing the more subtle but equally important barrier of increased spatial/temporal resolution. The larger scale motions in the ocean are mostly linear phenomena, albeit with complications discussed in the previous section, and nonlinearity arising from coupling with atmospheric phenomena, e.g. ENSO and the PDO. In contrast the mesoscale motions (dozens to a few hundreds of kilometers) are governed by nonlinear dynamics, characterized by strong self-interaction of oceanic eddies. Nonlinearity generically brings more complexity (Lorenz, 1963). Theoretical dynamical models since the 1970s predict a rich phenomenology (Charney 1971, Rhines 1975, McWilliams and Flierl, 1979, Salmon 1980, Hua and Haidvogel 1985, Treguier and Panetta, 1994, Jiang, Jin and Ghil, 1995, and many others) yet with only local and scant observational support. Only in the last few years has it been possible to observe the nonlinear phenomena and quantify their interactions.

Traditional altimeters in exact-repeat missions measure sea-surface height (SSH) along intersecting ground tracks. The regions between tracks form diamond patterns within which SSH is never sampled. Multiple altimeters operating simultaneously significantly improve the sampling. The degree to which this improves the resolution of SSH fields depends on the energy level of unresolved mesoscale variability, how well coordinated the orbit parameters are (repeat period, orbit inclination and measurement accuracy), the amount of spatial and temporal smoothing applied to the observations, and the subjectively chosen tolerance for residual errors (Chelton and Schlax, 2003). The residual errors for a given amount of smoothing can vary geographically and temporally in complicated ways, especially for small amounts of smoothing.

For a single satellite like Jason-2, constructed SSH fields have a resolution of about  $6^\circ$  in wavelength. The resolution is approximately doubled to about  $3^\circ$  for SSH fields constructed from observations from two altimeters (Jason-2 and ENVISAT), or even tripled to about  $2^\circ$  resolution with well-coordinated missions like Jason-2 and Jason-1 (Chelton and Schlax, 2003). For Gaussian eddies, these wavelength resolutions of  $6^\circ$ ,  $3^\circ$  and  $2^\circ$  correspond to e-folding eddy scales of 80 km, 60 km and 40 km, respectively. The above results apply to the smoothing procedure applied by AVISO (Ducet et al., 2000) to construct SSH fields from Jason-2 and ENVISAT and their predecessor combinations of one altimeter in a 10-day repeat orbit (TOPEX/Poseidon followed by Jason-1) and another altimeter in a 35-day repeat orbit (ERS-1 followed by ERS-2). The variability is attenuated for wavelengths shorter than about  $3^\circ$ , see also Pascual et al. (2006).

### i) *Propagating features*

The doubling of the spatial resolution of sea-surface height (SSH) fields constructed by AVISO (Ducet et al., 2000) from the merged measurements by two simultaneously operating altimeters (one in a 10-day repeat orbit and the other in a 35-day repeat orbit) has dramatically altered the earlier interpretation of westward propagating variability based on TOPEX/Poseidon data only. It is now evident that most of the extratropical variability at wavelengths of  $O(100-500\text{Km})$  that was thought to be linear baroclinic Rossby waves modified by the mean flow and bathymetry is actually westward propagating nonlinear eddies that are nearly ubiquitous in the World Ocean (upper panel of Fig. 2). The variability due to Rossby waves remains significant at wavelengths of  $O(1000\text{ Km})$  and longer.

An automated eddy tracking procedure identifies nearly 30,000 features with lifetimes of 16 weeks and longer. These observed features propagate nearly due west with small poleward and equatorward deflections of cyclonic and anticyclonic features, respectively, at approximately the speed of nondispersive baroclinic Rossby waves (Chelton et al., 2007). These propagation characteristics are consistent with theories for large, nonlinear eddies (McWilliams and Flierl, 1979). Additionally, zonal wavenumber-frequency spectra reveal little evidence of dispersion, again consistent with nondispersive eddy propagation (although Tailleux and Maharaj 2009 find nondispersion at high wavenumber due to mean flow effects).

The most telltale evidence that most of the observed features are nonlinear eddies is the predominance of large nonlinearity parameter  $U/c$ , where  $U$  is the maximum particle velocity within each feature and  $c$  is its translation speed. Features with  $U/c > 1$  contained trapped fluid. The average nonlinearity parameter exceeds 1 everywhere outside of the tropical band  $20^\circ\text{S}$  to  $20^\circ\text{N}$  (middle panel of Fig. 2). Moreover,  $U/c > 1$  for more than 90% of the extratropical eddies for both cyclones and anticyclones (bottom panels of Fig. 2). Even within the tropical band, more than 70% of the features are nonlinear.

The nonlinear character of the westward propagating features has important implications for ocean and climate dynamics. Unlike linear Rossby waves, nonlinear eddies can transport water properties over considerable distances. They also play a vital role in the energetics of ocean currents (Scott and Wang, 2005).

## ii) *Jets and zonal/meridional asymmetry*

On scales  $O(100\text{km})$  and  $O(1\text{week})$ , a combination of altimetry, drifter trajectories, and winds within a simplified momentum equation (Pascual et al. 2006; Maximenko and Niiler, 2005) provides an accurate description of mesoscale currents in the near-surface ocean. In this description, drifter data provide the absolute reference to the altimetry dataset, and altimetry corrects biases caused by the highly heterogeneous distribution of drifters. Thus-derived mean dynamic ocean topography (Maximenko et al., 2009) revealed complex frontal systems in the Antarctic Circumpolar Current, Gulf Stream, and Kuroshio Extension. In addition, a 'striped' global pattern of new jet-like features ('striations') was unveiled and validated using hydrographic data (Maximenko et al., 2008) (Fig. 3, below). While the nature and significance of these striations is not understood yet, the east-west tilt of the striations suggests stationary waves. Striations are also found in the altimetric sea level anomaly (Maximenko et al., 2005), which interact with eddies as strongly as the 'mean' striations. Eddies generated and moving along preferred paths may be involved (Scott et al., 2008, Schlax and Chelton, 2008), but this remains controversial (Maximenko et al., 2009, in prep.).

Scott et al. (2008) studied the anisotropy of the most energetic length scales, that are partially resolved by the high resolution sea surface height anomaly data from the constellation of at least three simultaneous satellite altimeters monitoring most of the ocean from year 2000 through 2005. They found mesoscale structure in the difference between the eastward and northward velocity variance throughout the extratropical World Ocean, qualitatively consistent with earlier results in the Southern Ocean (Morrow et al. 1994). The velocity variance structures are within the range of highly nonlinear eddy-eddy interactions. Contrary to the standard nonlinear model of the ocean mesoscale as homogenous quasigeostrophic turbulence (e.g. Arbic and Flierl 2004) the structures persist for years, i.e. much longer than the inherent timescales of quasigeostrophic turbulence. The pattern in velocity variance structures suggests an organizing mechanism yet the patterns are not simply related to bathymetry. The most important implications are likely to be the spatially variable and strongly anisotropic dispersion of tracers. Climate models may have to resolve the mesoscale explicitly since dispersion parameterization is likely a more formidable challenge than previously appreciated.

## iii) *Quantifying nonlinear interactions*

In the mesoscale, the flow becomes nonlinear and more complex, and theoretical models only make predictions for statistical flow properties. One of the most fundamental predictions is the so-called inverse energy cascade, in which the large scale flow gains energy from smaller scales via quasi-2D nonlinear interaction (e.g. Charney, 1971). The rate of this inverse cascade, called the spectral kinetic energy flux, was diagnosed as a function of length scale using multisatellite altimeter data, revealing a universal shape over the South Pacific that shifted to larger length scales closer to the Equator (Scott and Wang, 2005). Later analysis confirmed this universal shape throughout the World Ocean, see Fig. 4 below. The spectral flux divergence near the deformation radius suggested baroclinic instability near the deformation radius. This interpretation was later confirmed by comparing the regions of horizontal 2D wavenumber space that are baroclinically unstable, as computed with climatological temperature and salinity data,

and with spectral flux measurements computed with altimeter data (Qiu et al., 2008). These analyses provide the first observational evidence of the importance of beta (resulting from Earth's rotation and curvature) in redirecting the inverse cascade, as anticipated by Rhines (1975) and clarified by Vallis and Maltrud (1993) and Sukoriansky et al. (2007).

While the spectral flux measurements were inspired by classical quasi-2D turbulence theory, their observations required some theoretical developments for consistent interpretation. Classical theory predicts an inverse cascade for the barotropic (depth averaged) flow only, yet analysis of over 100 deep-water, long term, moored current meters spanning the water column suggests that most of the surface flow represents first mode baroclinic motions (vertically sheared flows with strongest signals in the upper ocean) (Wunsch, 1997). Thus the inverse cascade seen in altimeter data must imply an inverse cascade of baroclinic KE, a novel idea confirmed with idealized model simulations (Scott and Arbic, 2007).

### **C. Quantitative integration of multiple data types**

#### *i) Need for drifter data to complement altimeter data*

Altimeter data measure the time-varying geostrophic component of upper ocean velocities but cannot capture the time-mean velocity on mesoscales (since the geoid is only known on large scales) or the wind-forced ageostrophic velocity associated with Ekman (1905) dynamics. Surface drifter data are one way to measure total velocity, and are a valuable complement to altimeter data. Drifters have proved themselves as a useful measure of the time-invariant dynamic ocean topography (Niiler et al., 2003; Rio and Hernandez, 2003; Rio and Hernandez, 2004; Maximenko and Niiler, 2005, also Section B ii above), allowing detailed assessment of eddy mean flow interactions (e.g. Hughes and Ash, 2001; Hughes, 2005). In addition, differences between drifter and altimeter motions can be used to identify the transient ageostrophic velocity, providing insight into wind-forced motions of the upper ocean (e.g. Ralph and Niiler, 1999; Rio and Hernandez, 2003; Elipot and Gille, 2009). Drifters and other in situ data are invaluable for assessing errors in satellite derived surface currents (Johnson et al. ).

#### *ii) Critical role of scatterometer vector winds*

Upper ocean currents are wind-forced. Thus observations of winds play a critical role in the interpretation of the upper ocean currents measured by the altimeter. High-quality scatterometer estimates of wind speed and direction, measured relative to the moving ocean surface, have proved to be the most useful of available satellite wind products. Wind fields provide an estimate of the ageostrophic wind-driven upper ocean velocities that play an important role in advecting water within the upper ocean mixed layer (e.g. Ralph and Niiler, 1999; Rio and Hernandez, 2003; Dong et al., 2007, Bonjean and Lagerloef, 2002). Also, wind fields define the time-varying forcing of the ocean. As an example, the frontal features that define the Antarctic Circumpolar Current appear to migrate in response to changes in the latitude and character of the wind forcing over a variety of timescales (e.g. Dong et al., 2006; Sallée et al., 2008). Detailed analysis of the wind-forced evolution of ocean currents will require coincident high quality altimeter and scatterometer data. Previous estimates of the rate of wind work building the supply of available potential energy in the ocean all used NCEP reanalysis wind stress, which led to significant biases that were revealed and corrected with scatterometer winds (Scott and Xu,

2009).

iii) *Theoretical advances and observations of upper ocean dynamics*

Altimeter data, when analyzed in combination with surface drifter data and coincident wind observations, can provide detailed insights into upper ocean dynamics. For example, Rio and Hernandez (2003) used altimeter observations to separate geostrophic and ageostrophic motions measured by surface drifters and then inferred basic physical properties of the upper ocean: vertical viscosity and Ekman layer depth. Elipot and Gille (2009b) extended their approach, using the available observations to evaluate what functional form of upper ocean viscosity and what upper ocean boundary conditions would best explain the available observations.

## **PART II: REQUIRED TECHNOLOGICAL ADVANCEMENTS IN SATELLITE ALTIMETRY**

While satellite altimetry has substantially advanced our understanding of the ocean, we know that we are still missing a significant part of ocean variability associated with the submesoscale and smaller spatial scale variability. Dynamics and kinematics of this variability is believed to have a significant impact on ocean dynamics, especially on small-scale genesis, the interaction of coastal regions or frontal structures with the large-scale circulation, and also the interaction of the physical ocean with biology and biogeochemistry, as explained in more detail below. New technology is available to improve our observing capability of the mesoscale and to expand the sampling capabilities into the submesoscale and coastal domain, with an order of magnitude improvement in resolution.

We anticipate a direct societal benefit from further investment in ocean observing technology will come from supporting the development of ocean forecasting and longer term climate prediction. We are now able to produce simulations of the present state of the ocean that compare increasingly well to observations. However, the skill of these models in making long range predictions of the ocean is still limited, and will likely remain so, because they lack a physically based representation of the submesoscales, i.e. the more random motions on scales of 1-100 km (see the Nature editorial of May 15, 2008). Dissipation of momentum is achieved through enhanced vertical viscosities and drag laws with little physical validation. Turbulent transport of tracers like heat, salt, carbon and nutrients is represented with unphysical constant eddy diffusivities. Ocean models running at sufficient resolutions to address submesoscale dynamics have just begun to emerge (Capet et al., 2008), but we need global observations at these scales to guide model development.

### **A. New Technologies: Wide-swath altimetry and Delay-Doppler altimetry**

Surface Water Ocean Topography (SWOT) mission utilizes the new technology of a swath of width ~130 km (Fu and Rodriguez, 2004). This mission, if funded, will dramatically improve the resolution of SSH fields, allowing investigation of submesoscale variability with scales approximately an order of magnitude smaller than can presently be resolved from the merging of

observations from conventional altimeters. The SWOT mission was recommended recently by the National Research Council's Decadal Survey. Preliminary estimates of the performance of the SWOT measurement system indicate that measurement noise below 3 cm at 1/km sampling rate is within the range of the present technology. The noise spectra for 3 cm and 1 cm noise levels at 1/km sampling rate are plotted in Figure 5. If we extrapolate the SSH spectrum along the same power law from wavelengths longer than 100 km down to wavelengths of 1 km, we then find the intersection of the signal spectrum with the noise spectra at 30 km and 10 km wavelengths for 3 cm and 1 cm noise level, respectively. In order to resolve the narrow currents and fronts in the ocean, we must resolve signals at wavelengths down to 10 km, pushing the measurement requirement to a noise level of 1 cm at 1/km sampling rate, compared to the noise of 5 cm at 1/km sampling rate for the Jason altimeter. This performance in SSH measurement translates to a geostrophic velocity error of 3 cm/sec at 10 km wavelength at 45° latitude. The two dimensional SSH map from SWOT will observe these features and will thereby allow the study of the submesoscale ocean eddies, fronts, narrow currents, and even the vertical velocity at these scales. However, to capture related temporal variability one would still need more than one SWOT mission.

Nadir-pointing along-track altimetry is also about to undergo a dramatic improvement, which will be made possible by the adoption of delay-Doppler processing of the echo returns. Delay-Doppler altimetry (DDA) was proposed in the 1990s (Raney, 1998) as a more efficient alternative to conventional altimetry. DDA uses the Doppler information contained in the returns (and essentially due to the satellite motion with respect to the surface) to resolve iso-Doppler subregions within the area illuminated by each altimetric pulse; therefore it allows an integration of the contributions coming from a large number of multiple looks on the same along-track Doppler cell. The result is either a much higher along-track resolution (the along-track cell is of the order of a few hundred meters; across track it is limited by the antenna beamwidth so of  $O(10\text{km})$ ), or an improved signal to noise ratio (possible by averaging several independent along-track cells), or any intermediate trade off between enhanced resolution and enhanced SNR. Another beneficial characteristic is a reduced sensitivity of the measurements on the sea state. The first DDA in space will be the CryoSat-2 altimeter due to be launched in late 2009, and ESA is going to adopt the DD paradigm also for the Sentinel-3 altimeter, successor to the ERS and Envisat instruments. The combination of improved resolution and precision of this new family of instruments holds great promise for observations of the submesoscale; moreover they are expected to give a significant contribution to the emerging field of coastal altimetry (see the CWP by Cipollini et al., 2009)

## **B. Potential breakthroughs in ocean dynamics and biogeochemistry**

Global observations of the oceanic submesoscale are essential to quantifying the ocean uptake of climate relevant tracers such as heat and carbon. Traditional altimeters revealed the fundamental role of mesoscale eddies in the horizontal transport of tracers. Recent theoretical work suggests that submesoscale motions play a leading role in the vertical transport (Lapeyre et al., 2006; Boccaletti et al., 2007; Capet et al., 2008, Klein et al. 2008). Vertical velocities in the ocean require higher spatial resolution because they result from convergences and divergences in the horizontal velocity field. Submesoscale motions at the ocean surface are a superposition of Ekman velocities, driven by the wind, and geostrophic velocities. Scatterometers provide



detailed measurements of the wind stress field and allow estimates of the wind-driven vertical velocities. First attempts (Lapeyre and Klein, 2006; LaCasce and Mahadevan, 2006) to reconstruct the 3D circulation in the first 300m from climatological data and high-resolution SST are quite promising. However the high resolution SSH of wide-swath interferometry is necessary to bring the approach to full fruition and provide global maps of the vertical velocities associated with geostrophic motions. Our understanding of the ocean and its role in climate would be radically advanced should such maps become available.

Attempts to further diagnose the oceanic circulation in a realistic situation involving a mesoscale eddy field with large Rossby numbers and an active mixed-layer forced by high frequency winds have been recently achieved (Klein et al., 2009). Results (see Fig. 6) reveal that, despite the presence of energetic near-inertial motions, a snapshot of high resolution SSH allows reconstruction of low frequency motions, including the vertical velocities, for scales between 400km and 20km and depths between the mixed-layer base and 500m. As such these results highlight the potential of high-resolution SSH to assess in the upper ocean the low frequency horizontal and vertical fluxes of momentum and tracers driven by mesoscale and submesoscale dynamics. Some work still to be done to improve this simple diagnosis method includes its testing in a broader range of mesoscale eddy and mixed-layer regimes and its improvement to diagnose the specific mixed-layer dynamics.

The uptake of heat and carbon by the ocean is complete only after these properties are transported away from the surface turbulent boundary layer into the ocean interior. Vertical velocities associated with divergences and convergences of geostrophic balanced velocities on 10 km scale penetrate down to a few hundred meters below the ocean surface (Lapeyre et al., 2006). Hence the resolution of SWOT will allow one to compute the exchange of properties between the ocean surface boundary layers and the interior. Furthermore these measurements will be fundamental to improving the skills of coupled climate models that are very sensitive to the exchange of properties between the ocean and the atmosphere.

Another application of the SSH measurements at the submesoscale is for estimates of biological productivity. Ocean colour is very often characterized by a web of filaments of enhanced biological activity. It is impossible from a surface picture to determine whether these filaments are associated with lateral stirring of biomass or with new productivity resulting from vertical advection of new nutrients into the filaments. The distinction is crucial for the global carbon cycle; the latter case implies an enhancement of the biological carbon pump. Therefore the SWOT mission could contribute essential new information to further our understanding of the submesoscale physics and biology of the upper ocean.

### **Part III: Integrating emerging technologies while maintaining existing technologies**

Most climate records have been obtained as the by-product of measurements made for a different purpose, especially weather observations, and commonly it is asserted that simply sustaining these networks is the surest way to determining changes in climate. This approach often generates some very great and intractable difficulties. By some arguments, the sustenance of high quality, sometimes demanding, but nonetheless routine, measurements are the most difficult

of all to obtain and for many reasons. Each oceanographic data type is in need of constant supervision by technically qualified scientists who can determine if standards are being followed, that calibration protocols have been adhered to, and is in a position to influence a decision to change a data type. Because the intellectual payoff of many records might be decades in the future, incentives have to be provided for scientists to invest their time and energies into efforts with little personal gratification other than a sense of doing a service to the community.

Many examples of difficult decisions about technology change abound. Therefore, given those experiences, we should continue TOPEX-Jason class even when the next generation of altimeters will be of the swath type. (Note that there are remaining calibration discrepancies between even these instruments.) Only if we can assume the indefinite existence of high quality altimeters, the tide gauge network could be thinned. On the other hand, in situ data are essential for calibrating data from individual altimeter missions. In addition, sea level has proven to vary on small coastal scale and to monitor sea level changes we might even need to expand the existing tide gauge network. Argo floats should be made to reach the sea floor. It needs to be investigated to what extend the surface observing system could be thinned then, but at this point no indication exists that the ocean is oversampled – just the opposite. In the same vain we need to investigate whether scatterometers should completely replace the surface anemometer network apart from a few very high quality calibration positions. These questions will need to be answered before we can decide what kind of investment should be made in meteorological buoys. These are difficult problems that cannot be relegated to uninterested committees for solution. To answer them requires a serious and quantitative design study of the observing system, which addresses also uncertainties in the observations, the models and the estimates that we obtain by bringing observations and models together. An ocean observing system that is intended to truly address climate change must have a scientific supporting infrastructure that is in constant control of the system.

## References:

- Arbic, B.K. and Flierl, G.R. 2004: Effects of mean flow direction on energy, isotropy, and coherence of baroclinically unstable beta-plane geostrophic turbulence, *J. Phys. Oceanogr.*, Vol. 34, pp. 77—93.
- Boccaletti G., R. Ferrari, and B. Fox-Kemper, 2007: Mixed Layer Instabilities and Restratification, *J. Phys. Oceanogr.*, 37, 2228-2250.
- Bonjean, F., and G.S.E. Lagerloef, 2002: Diagnostic model and analysis of the surface currents in the tropical Pacific Ocean, *J. Phys. Oceanogr.*, 32, 2938-2954.
- Capet, X., J.C. McWilliams, M.J. Molemaker, and A.F. Shchepetkin, 2008: Mesoscale to submesoscale transition in the California Current System. Part I: Flow structure, eddy flux, and observational tests. *J. Phys. Oceanogr.*, Vol. 38, 29-43.
- Charney, J.G. 1971: Geostrophic Turbulence, *J. Atmos. Sci.* Vol. 28, pp. 1087—1095.
- Chelton DB and Schlax MG, 1996: Global observations of oceanic Rossby waves, *Science*, Volume: 272 Issue: 5259 Pages: 234-238.
- Chelton, D. B., M. G. Schlax, R. M. Samelson, and R. A. de Szoeke, 2007: Global observations of large oceanic eddies. *Geophys. Res. Lett.*, 34, L15606, doi:10.1029/2007GL030812.
- Cipollini, P. + 18 co-auhtors, 2009: “The Role of Altimetry in Coastal Observing Systems”, *OceanObs’09 Community White Paper*.
- Deser, Clara, Michael A. Alexander And Michael S. Timlin,1999: Evidence for a Wind-Driven Intensification of the Kuroshio Current Extension from the 1970s to the 1980s , *J. Clim.*, Vol. 12, pp. 1697—1706.
- Dong, S., J. Sprintall, and S. T. Gille, 2006: Location of the Polar Front from AMSR-E satellite sea surface temperature measurements, *J. Phys. Oceanogr.*, 36, 2075-2089.
- Dong, S., S. T. Gille, J. Sprintall, 2007: An assessment of the Southern Ocean mixed-layer heat budget, *J. Climate*, 20, 4425-4442.
- Ducet, N., P.-Y. Le Traon, and G. Reverdin, 2000: Global high resolution mapping of ocean circulation from TOPEX/POSEIDON and ERS-1/2. *J. Geophys. Res.*, 105, 19,477-19,498.
- Elipot, S. and S. T. Gille, 2009a: Estimates of wind energy input to the Ekman layer in the Southern Ocean from surface drifter data, accepted by *J. Geophys. Res.*

Elipot, S. and S. T. Gille, S. T., 2009b: Ekman layers in the Southern Ocean: spectral models and observations, vertical viscosity and boundary layer depth, submitted Ocean Sci. Discuss., 6, 277-341.

Fu, L.-L., and A. Cazenave, editors, 2001: Satellite Altimetry and Earth Sciences: A Handbook of Techniques and Applications., Academic Press, San Diego, 463 pp.

Fu LL and Chelton DB 2001: Large-scale Ocean circulation. In ``Satellite altimetry and Earth Sciences'', Fu and Cazenave editors, International Geophysics Series. Volume 69. Pages: 133-165

Fu, L.-L., and R. Ferrari (2008): Observing Oceanic Submesoscale Processes From Space, *Eos Trans. AGU*, 89(48), doi:10.1029/2008EO480003.

Fu, L.-L., and R. Rodriguez, 2004: High-resolution measurement of ocean surface topography by radar interferometry for oceanographic and geophysical applications, AGU Geophysical Monograph 150, IUGG Vol. 19: "State of the Planet: Frontiers and Challenges", R.S.J. Sparks and C.J. Hawkesworth, editors, 209-224.

Hua, B.L. and Haidvogel, D. 1986: Numerical simulations of the vertical structure of quasi-geostrophic turbulence, *J. Atmos. Sci.*, Vol. 43, pp. 2923—2936.

Hughes, C. W. and Ash E. R., 2001: Eddy forcing of the mean flow in the Southern Ocean, *J. Phys. Oceanogr.*, 31(10), pp.2871-2885.

Hughes, C. W., 2005: Nonlinear vorticity balance of the Antarctic Circumpolar Current, *J. Geophys. Res.*, 110, C11008, doi:10.1029/2004JC002753.

Jiang, S., F. Jin and M. Ghil, 1995: Multiple equilibria, Periodic and Aperiodic solutions in a wind-driven, double-gyre, shallow-water model, *J. Phys. Oceanogr.*, Vol. 25, pp. 764—786.

Johnson, E.S., F. Bonjean, G.S.E. Lagerloef, J.T. Gunn, and G. T. Mitchum, 2007: Validation and Error Analysis of OSCAR Sea-surface Currents, *J. of Atmospheric and Oceanic Technology*, 24(4), 688-701.

Killworth PD, Chelton DB, de Szoeki RA, 1997: The speed of observed and theoretical long extratropical planetary waves. *J. Phys. Oceanogr.* Volume: 27 Issue: 9 Pages: 1946-1966.

Killworth PD and Blundell JR, 2003: Long extratropical planetary wave propagation in the presence of slowly varying mean flow and bottom topography. Part II: Ray propagation and comparison with observations. *J. Phys. Oceanogr.* Volume: 33 Issue: 4 Pages: 802-821.

Killworth PD and Blundell JR, 2003: Long extratropical planetary wave propagation in the presence of slowly varying mean flow and bottom topography. Part I: The local problem. *J. Phys. Oceanogr.* Volume: 33 Issue: 4 Pages: 784-801.

Killworth PD and Blundell JR, 2004: The dispersion relation for planetary waves in the presence of mean flow and topography. Part I: Analytical theory and one-dimensional examples. *J. Phys. Oceanogr.* Volume: 34 Issue: 12 Pages: 2692-2711.

Killworth PD and Blundell JR, 2005: The dispersion relation for planetary waves in the presence of mean flow and topography. Part II: Two-dimensional examples and global results. *J. Phys. Oceanogr.* Volume: 35 Issue: 11 Pages: 2110-2133.

Kistler, R. E., Kalnay, E. M. W. Collins, S. Saha, G. White, J. Woollen, M. Chelliah, W. Ebisuzaki, M. Canamitsu, V. Kousky, H. van den Dool, R. Jenne and M. Fiorino, 2001: The NCEP/NCAR 50-year reanalysis: Monthly means CD-ROM and documentation, *Bull. Amer. Met. Soc.*, Vol. 82, pp. 247—267.

Klein, P., Hua B.L., G. Lapeyre, X. Capet, S. LeGentil and H. Sasaki., 2008: Upper Ocean Dynamics from High 3-D Resolution Simulations. *J. Phys. Oceanogr.*, 38, pp. 1748–1763.

Klein et al. , 2009: Diagnosis of vertical velocities in the upper ocean from high resolution Sea Surface Height, submitted to *Geophys. Res. Letters*.

Lapeyre, G., P. Klein, and B. L. Hua, 2006: Oceanic restratification forced by surface frontogenesis. *J. Phys. Oceanogr.*, 36, 1577-1590.

Lapeyre, G., and P. Klein, 2006: Dynamics of upper oceanic layers in terms of surface quasigeostrophic theory. *J. Phys. Oceanogr.*, 36, 165-176.

LaCasce, J. H. and A. Mahedavan, 2006: Estimating sub-surface horizontal and vertical velocity from sea surface temperature. *J. Mar. Res.*, 64, 695-721.

Lorenz, E. 1963: Deterministic nonperiodic flow, *J. Atmos. Sci.*, Vol. 20, pp. 130—141.

Maharaj AM, Holbrook NJ, and Cipollini, P: An assessment of multiple westward propagating signals in sea level anomalies. Submitted to *J. Geophysical Research*.

Mantua, N. J., S. R. Hare, Y. Zhang, J. M. Wallace and R. C. Francis (1997): A Pacific interdecadal climate oscillation with impacts on salmon production. *Bull. Amer. Meteor. Soc.*, 78, 1069–1079.

Maximenko, N. A. and P. P. Niiler, 2005: Hybrid decade-mean global sea level with mesoscale resolution, in *Recent Advances in Marine Science and Technology, 2004*, ed. by N. Saxena, Honolulu: PACON International, pp. 55-59.

Maximenko, N., P. Niiler, M.-H. Rio, O. Melnichenko, L. Centurioni, D. Chambers, V. Zlotnicki, and B. Galperin, 2009: Mean dynamic topography of the ocean derived from satellite and drifting buoy data using three different techniques. *J. Atmos. Oceanic Tech.*, accepted.

Maximenko, N.A., O. V. Melnichenko, P. P. Niiler, and H. Sasaki, 2008: Stationary mesoscale jet-like features in the ocean. *Geophys. Res. Lett.*, 35, L08603, doi:10.1029/2008GL033267.

Maximenko, N.A., B. Bang, and H. Sasaki, 2005: Observational evidence of alternating zonal jets in the World Ocean. *Geophys. Res. Lett.*, 32, L12607, doi:10.1029/2005GL022728.

Maximenko, N.A., and P.P. Niiler, 2005: Hybrid decade-mean global sea level with mesoscale resolution. In N. Saxena (Ed.) *Recent Advances in Marine Science and Technology*, 2004, pp. 55-59. Honolulu: PACON International.

Maximenko, N. A., O. V. Melnichenko, and H.-P. Huang, 2009: Are oceanic striations an artifact of moving eddies? In prep.

McWilliams, J. C., and G. R. Flierl (1979): On the evolution of isolated, nonlinear vortices, *J. Phys. Oceanogr.*, 9, 1155-1182.

Miller, A. J., D. R. Cayan, and W. B. White, 1998: A westward intensified decadal change in the North Pacific thermocline and gyre-scale circulation. *J. Climate*, 11, 3112–3127.

Morrow, R.A., R. Coleman, J.A Church, and D.B. Chelton, 1994: Surface eddy momentum flux and velocity variances in the Southern Ocean from Geosat altimetry. *J. Phys. Oceanogr.*, 24, 2050-2071.

Nature, editorial 2008: “The next big climate challenge”. *Nature*, Vol. 453, Issue no. 7193, p. 257.

Niiler, P. P. and N. A. Maximenko and J. C. McWilliams, 2003: Dynamically balanced absolute sea level of the global ocean derived from near-surface velocity observations, *Geophys. Res. Lett.*, 30:22, 2164, doi:10.1029/2003GL018628.

Pascual, A., Faugere, Y., G. Larnicol, P.Y. Le Traon, 2006: Improved description of the ocean mesoscale variability by combining four satellite altimeters. *Geophys. Res. Letters*, 33 (2): Art. No. L02611.

Qiu, B. and S. Chen 2005: Variability of the Kuroshio Extension Jet, Recirculation Gyre, and Mesoscale Eddies on Decadal Time Scales, *J. Phys. Oceanogr.*, Vol. 35, pp. 2090—2103.

Qiu, B., R.B. Scott, and S. Chen, 2008: Length-scales of generation and nonlinear evolution of the seasonally-modulated South Pacific Subtropic Countercurrent, *J. Phys. Oceanogr.*, Vol. 38, pp. 1515—1528.

Ralph, E. A. and P. P. Niiler, 1999: Wind-driven currents in the tropical Pacific, *J. Phys. Oceanogr.*, 29, pp. 2121--2129.

Raney, R. K., 1998: The delay Doppler radar altimeter, *IEEE Transactions on Geoscience and Remote Sensing*, vol. 36, pp. 1578-1588.

- Rhines, P. 1975: Waves and turbulence on a beta-plane, *J. Fluid Mech.*, Vol. 69, pp. 417—443.
- Richman, J.G., C. Wunsch, and N.G. Hogg, 1977: Space and time scales and mesoscale motion in the sea. *Rev. Geophys. Space Phys.*, 15, 385-420.
- Rio, M.-H. and F. Hernandez, 2003: High frequency response of wind-driven currents measured by drifting buoys and altimetry over the world ocean, *J. Geophys. Res.*, 108(C8), 3283, doi:10.1029/2002JC001655.
- Rio, M. H. and F. Hernandez, 2004: A mean dynamic topography computed over the world ocean from altimetry, in situ measurements, and a geoid model, *J. Geophys. Res.*, 109, C12032, doi:10.1029/2003JC002226.
- Robinson, A.R., 1983: editor, *Eddies in Marine Science*, Springer-Verlag, 609 pp.
- Sallée, J.-B., K. Speer, and R. Morrow, 2008: Southern Ocean fronts and their variability to climate modes, *J. Climate*, 21(12), 3020-3039.
- Salmon, R. 1980: Baroclinic Instability And Geostrophic Turbulence, *Geophys. Astrophys. Fluid Dyn.*, Vol. 15, pp. 167—211.
- Schneider, N., A. J. Miller, and D. W. Pierce, 2002: Anatomy of North Pacific decadal variability. *J. Climate*, 15, 586–605.
- Scott, R.B. and B.K. Arbic 2007: Spectral energy fluxes in geostrophic turbulence: implications for ocean energetic, *J. Phys. Oceanogr*, Vol. 37, pp. 673—688.
- Scott, R.B. and F. Wang 2005: Direct evidence of an oceanic inverse kinetic energy cascade from satellite altimetry, *J. Phys. Oceanogr*, Vol. 35, pp. 1650—1666.
- Scott, R.B. and Xu, Y. 2009: An update on the wind power input to the surface geostrophic flow of the World Ocean, *Deep Sea Research I*, Vol. 56, pp. 295—304.
- Seager, R., Y. Kushnir, N. H. Naik, M. A. Cane, and J. Miller, 2001: Wind-driven shifts in the latitude of the Kuroshio–Oyashio extension and generation of SST anomalies on decadal timescales. *J. Climate*, 14, 4249–4265.
- Schlax, Michael G. and Dudley B. Chelton, 2008: The influence of mesoscale eddies on the detection of quasi-zonal jets in the ocean, *Geophys. Res. Lett.*, VOL. 35, L24602, doi:10.1029/2008GL035998.
- Smith, R.D., Maltrud, M.E., Bryan, F.O., and Hecht, M.W., 2000: Numerical simulation of the North Atlantic ocean at  $1/10^\circ$ . *J. Phys. Oceanogr.*, 30, 7,1532–1561.
- Sokolov, S. and Rintoul, S.R., 2007: Multiple jets of the Antarctic Circumpolar Currents south of Australia. *J Phys Oceanogr* 37:1394–1412.

Sukoriansky, S., N. Dikovskaya, and B. Galperin, 2007: On the 'arrest' of the inverse energy cascade and the Rhines scale, *J. Atm. Sci.*, 64, 3312–3327.

Taguchi et al. Decadal Variability of the Kuroshio Extension, 2007: Observations and an Eddy-Resolving Model Hindcast, *J. Clim.* Vol. 20, pp. 2357—2377.

Tailleux R and McWilliams, JC, 2001: The effect of bottom pressure decoupling on the speed of extratropical, baroclinic Rossby waves. *J. Phys. Oceanogr.*. Volume: 31 Issue: 6 Pages: 1461-1476

Tailleux R and McWilliams, JC, 2002: Energy propagation of long extratropical Rossby waves over slowly varying zonal topography. *J. Fluid Mech.* Volume: 473 Pages: 295-319

Tailleux, R, 2006: The quasi-nondispersive regimes of long extratropical baroclinic rossby waves over (slowly varying) topography. *J. Phys. Oceanogr.* Volume: 36 Issue: 1 Pages: 104-121.

Tailleux R and Maharaj AM, 2009: On the zonal wavenumber/frequency spectrum of westward propagation. Part I: Theory. To be submitted.

Treguier, A. and L. Panetta, 1994: Multiple Zonal Jets in a Quasigeostrophic Model of the Antarctic Circumpolar Current, *J. Phys. Oceanogr.*, Vol. 24, pp. 2263—2277.

Vallis, G.K. and M. Maltrud, 1993: Generation of mean flows and jets on a beta plane and over topography, *J. Phys. Oceanogr.*, Vol. 23, pp. 1346—1362.

Wunsch, C. 1997: The vertical partition of oceanic horizontal kinetic energy and the spectrum of global variability, *J. Phys. Oceanogr.*, Vol.27, pp. 1770—1794.



## Figures

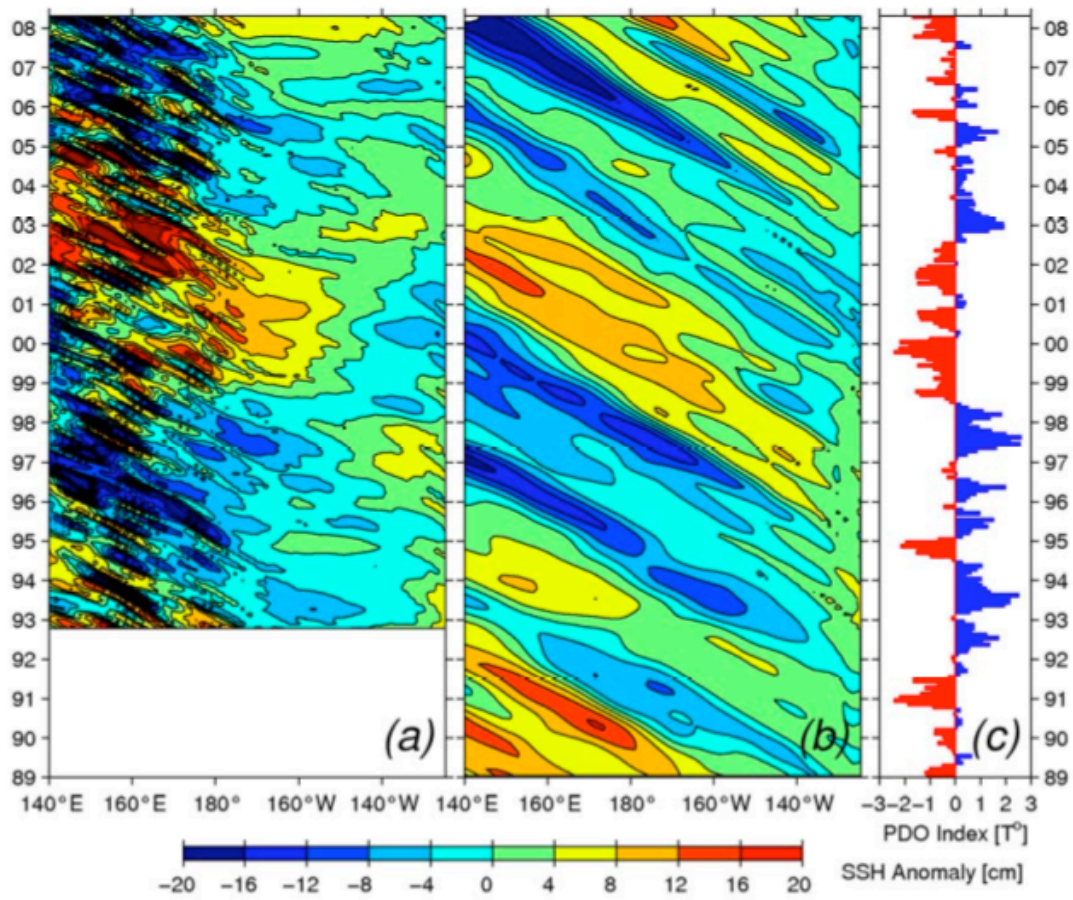


Figure 1: (a) SSH anomalies along the zonal band of 32-34°N from the satellite altimeter data. (b) Same as panel a but from the wind-forced baroclinic Rossby wave model. (c) PDO index from <http://jisao.washington.edu/pdo/PDO.latest>.

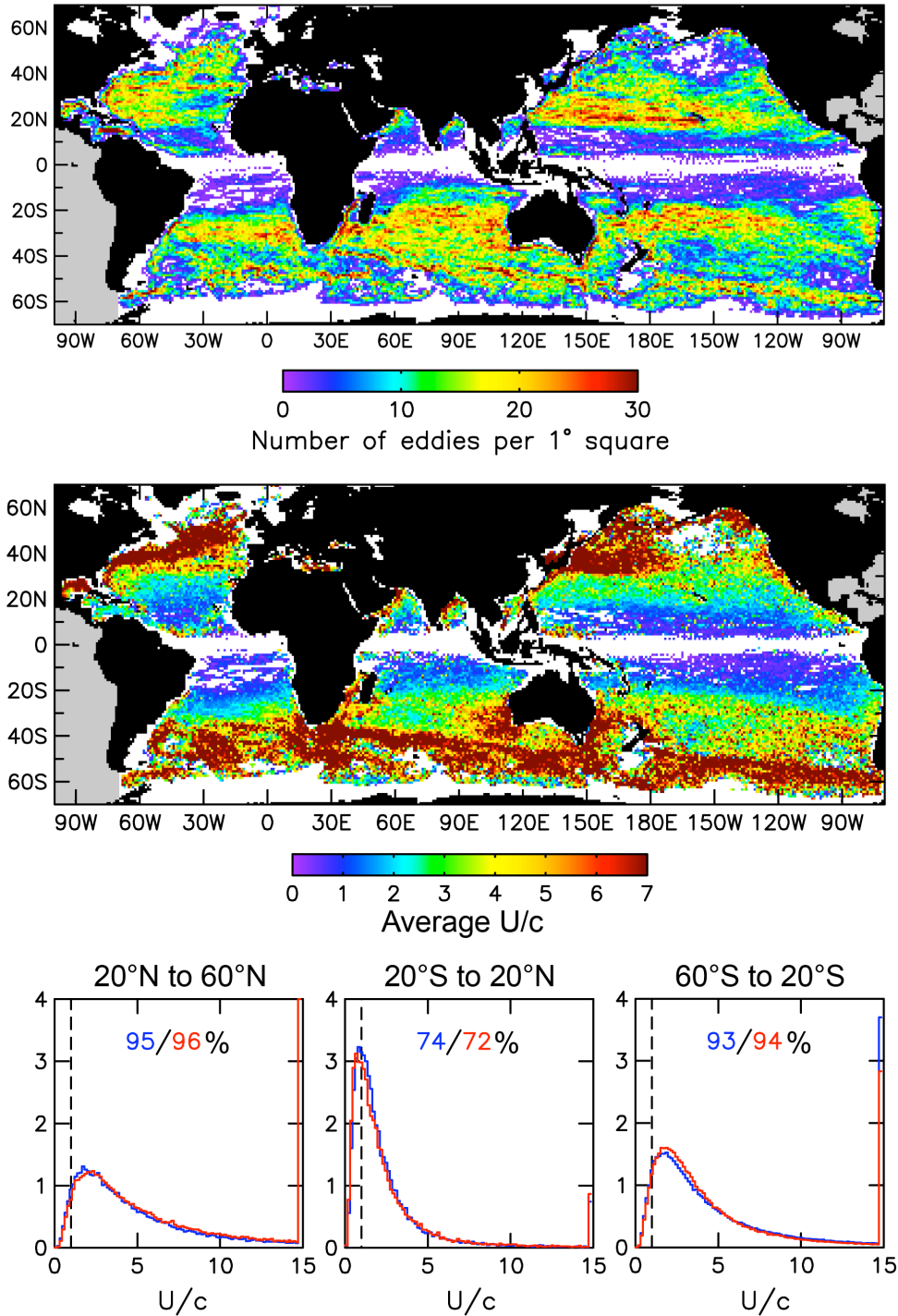


Figure 2: The characteristics of features tracked for 16 weeks and longer over a 14-year data record of merged measurements from two simultaneously operating altimeters (Ducet et al., 2000). Upper: The number of eddy centres per 1° square over the 14-year data record. Middle: The average nonlinearity parameter  $U/c$  in each 1° square. Bottom: The distributions (in percent) of the nonlinearity parameter  $U/c$  for the observed features in three different latitude bands.

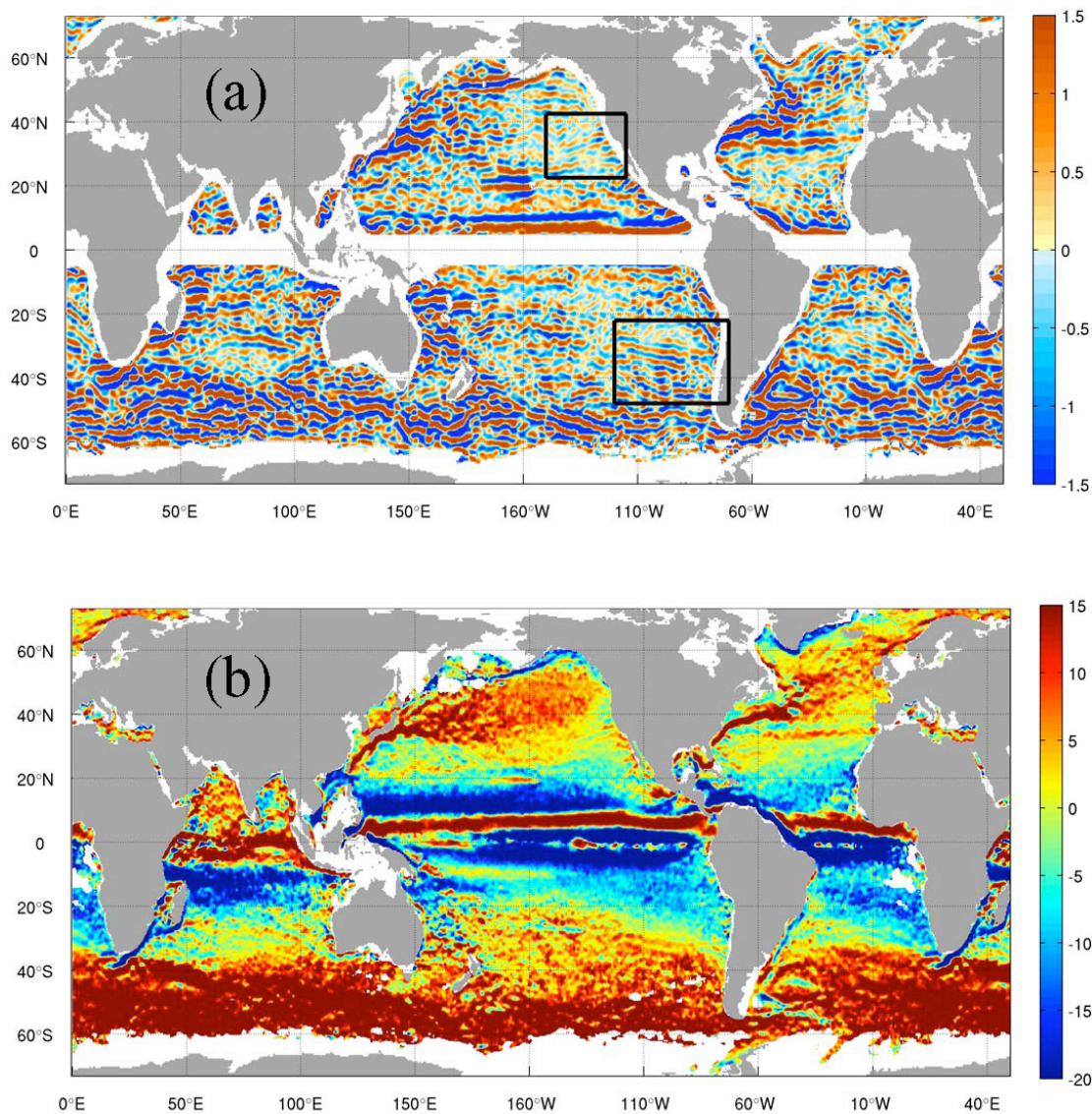


Figure 3: (a) 1993-2002 mean zonal surface geostrophic velocity calculated from the MDOT of Maximenko and Niiler (2005) high-pass filtered with a two-dimensional Hanning filter of 4° half-width. (b) Ensemble-mean zonal velocity calculated from the data of AOML. Rectangles in (a) outline two study domains where striations are validated by historical XBT data. Units are cm/s. (Figure from (Maximenko et al., 2008).)

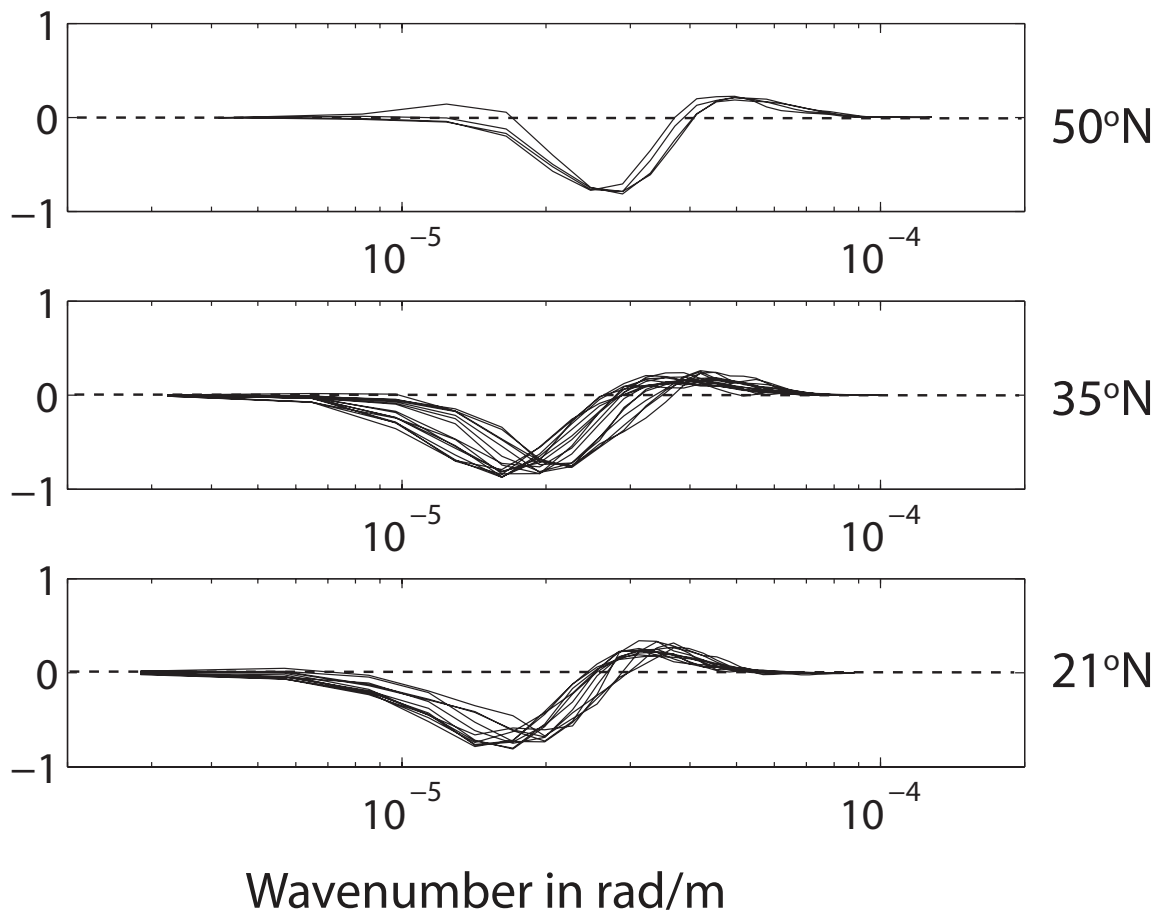


Figure 4: Spectral kinetic energy flux, normalized by its peak to peak amplitude, vs. wavenumber, calculated from multi-satellite altimeter data on square boxes with width  $22^\circ$  longitude throughout the Northern Hemisphere. Similar results found in the Southern Hemisphere.

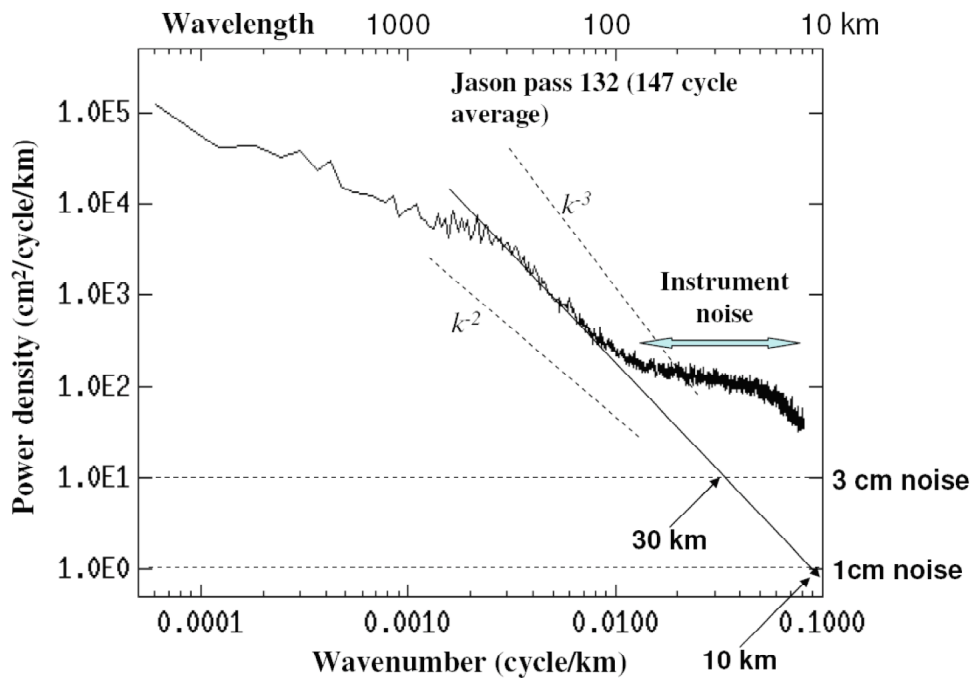


Figure 5: Wavenumber spectrum of sea surface height anomaly from 147 repeat measurements along Jason pass 132 (solid line). The two slanted dashed lines represent two spectral power laws with  $k$  denote wavenumber. The two horizontal dashed lines represent two levels of measurement noise at 1/km sampling rate: 3 cm and 1 cm. The slanting solid straight line represents a linear fit of the spectrum in the range between 0.002 and 0.01 cycles/km. It intersects with the two noise level lines at 30 km and 10 km wavelengths.

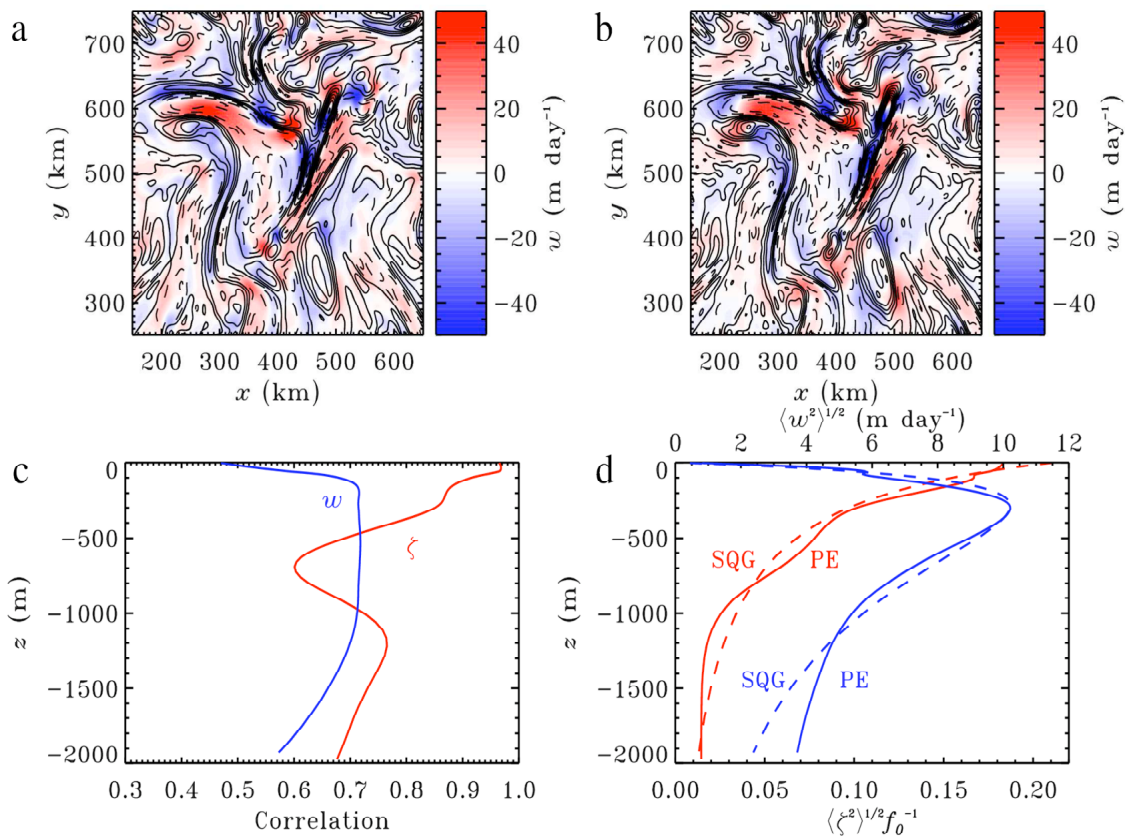


Figure 6: a) Observed low-frequency vertical velocity (in colors) and relative vorticity (contours) at 200 m. b) eSQG reconstructed vertical velocities (in colors) and relative vorticity (contours) at 200 m. c) Correlation between observed and eSQG reconstructed vertical velocities (blue line) and relative vorticity (red line). d) Vertical velocities RMS (blue) and relative vorticity RMS (red) observed in the PE simulation (solid line) and reconstructed using eSQG (dashed line).